



# Assessment of facial autologous fat grafts using Dixon magnetic resonance imaging

Xueyin Liao<sup>1</sup>, Xiaoqi Wang<sup>2</sup>, Zhentan Xu<sup>3</sup>, Shiwei Guo<sup>1</sup>, Congmin Gu<sup>1</sup>, Zhengyu Jin<sup>3</sup>, Tong Su<sup>3</sup>, Yu Chen<sup>3</sup>, Huadan Xue<sup>3</sup>, Mingyong Yang<sup>1</sup>

<sup>1</sup>Plastic Surgery Hospital, Chinese Academy of Medical Sciences and Peking Union Medical College, Beijing, China; <sup>2</sup>Philips Healthcare, the World Profit Centre, Beijing, China; <sup>3</sup>Department of Radiology, Peking Union Medical College Hospital, Chinese Academy of Medical Sciences, Beijing, China

*Contributions:* (I) Conception and design: Y Chen, H Xue, M Yang; (II) Administrative support: Y Chen, H Xue, M Yang; (III) Provision of study materials or patients: X Liao, X Wang, Y Chen, Z Xu, T Su; (IV) Collection and assembly of data: X Liao, X Wang, C Gu, S Guo; (V) Data analysis and interpretation: X Liao, X Wang; (VI) Manuscript writing: All authors; (VII) Final approval of manuscript: All authors.

*Correspondence to:* Yu Chen, MD. Department of Radiology, Peking Union Medical College Hospital, Chinese Academy of Medical Sciences, No.1 Shuai Fu Yuan, Dong Cheng District, Beijing 100730, China. Email: bjchenyu@126.com; Huadan Xue, MD. Department of Radiology, Peking Union Medical College Hospital, Chinese Academy of Medical Sciences, No.1 Shuai Fu Yuan, Dong Cheng District, Beijing 100730, China. Email: bjdanna95@163.com; Mingyong Yang, MD. Plastic Surgery Hospital, Chinese Academy of Medical Sciences and Peking Union Medical College, 33 Badachu Road, Shijingshan District, Beijing 100144, China. Email: yangmy2005@163.com.

**Background:** Autologous fat grafting is a procedure that treats soft tissue defects by reallocating fat to improve a patient's physical appearance. Imaging methods may be used to evaluate and monitor the grafted fat after transplantation. The goal of imaging is to examine the signal and volume of the grafted fat after autologous fat grafting during the adipose tissue recovery. However, researchers have yet to examine the feasibility of using fat-only imaging to assess the autologous fat graft.

**Methods:** In this prospective and observational study, 46 injected sides in 23 female patients (age 35±7.8 years) were included in the image evaluation. The patients underwent autologous fat grafting surgery with filtered and washed fat. A total of 16, 18, and 12 sides were scanned 7 days, 3 months, and 1 year after fat grafting, respectively. Fat-only images were obtained using Dixon imaging, and then the image quality and contrast of the T1W and T2W were rated to evaluate the application of this method when imaging the autologous fat. The signal and volume of the autologous fat graft were recorded to assess the retention during recovery of the autologous fat tissue.

**Results:** Fat-only T1W magnetic resonance imaging (MRI) was used to identify and delineate grafted fat because this method had better image quality and image differentiation than did T2W MRI. The average signal contrast and retention rate measured 7 days postoperation (28.8%±4.7%; 94.1%±5.8%) was the highest and then decreased at 3 months (16.3%±2.1%; 48.7%±17.3%) and 1 year (3.3%±1.3%, 33.1%±12.9%) after surgery. There were statistically significant differences between the signal and volume retention measurements at each postoperative recovery phase.

**Conclusions:** The T1W fat-only images produced by Dixon MRI is a feasible approach for identifying grafted fat and measure postoperative changes during clinical evaluation. We found a significant decrease in signal contrast and volume of the grafted fat from the surgery date to 3 months postoperation and from 3 months to 1-year postoperation.

**Keywords:** Facial fat transplantation; autologous fat graft; magnetic resonance imaging (MRI); chemical shift; Dixon

Submitted May 29, 2021. Accepted for publication Jan 24, 2022.

doi: 10.21037/qims-21-570

View this article at: <https://dx.doi.org/10.21037/qims-21-570>

## Introduction

Aging, trauma, and diseases can cause soft tissue defects, which can be treated with various filling materials to improve a patient's physical appearance (1). Fat grafting is a process that reallocates fat from the thighs or abdomen to the defect region, allowing good tissue compatibility with a minimized rate of tissue rejection and no allergic reaction (2). Surgeons use this procedure in facial rejuvenation, lipoatrophy (3-5), and breast and glutes augmentation (6-10). Researchers have assessed the surgical outcomes by measuring the autologous fat graft's long-term volumetric retention in improving surgical procedures and the survival rate of grafted fat (1,11). Noninvasive imaging methods, including ultrasound, computed tomography (CT), 3D facial scanner, and conventional magnetic resonance imaging (MRI), have been applied in previous studies to assess fat graft retention; however, the inaccuracy or insensitivity in such modalities limits their applications for the face due to its small volume (8,11,12). For example, ultrasound imaging applies pressure on soft tissue that changes the tissue's shape, and the thick layer of the water-based gel used for ultrasound transmission between the probe and skin is not suitable in cosmetic surgery clinics (1). CT images do not offer sufficient contrast to distinguish autologous fat graft from subcutaneous fat (13). More importantly, ionizing radiation from the X-ray during CT inhibits its broad application. Moreover, previous studies using a fat suppression MRI sequence also found it difficult to delineate grafted fat (1,4,7).

The Dixon sequence can be implemented using various sequence implementation and reconstruction algorithms (14-19). The mechanism of the Dixon sequence is based on the chemical shift effect, which separates the water and fat signal (20). Although the in-phase and water-only (fat-suppressed) images generated by Dixon imaging are commonly used for clinical diagnosis (21,22), the fat-only image has not been frequently used. Fat-only images are usually discarded except in fat quantification measurements, but they provide high-quality anatomical images of adipose tissue without requiring a contrast agent or additional image postprocessing.

We hypothesized that fat-only images could provide

visualization of grafted fat following the autologous fat transfer and guide the second injection procedures. This study aimed to assess the application of Dixon imaging's fat-only image when characterizing autologous fat graft and to assess the changes of the grafted fat signal and its volume retention within 1 year after surgery.

We present the following article in accordance with the MDAR checklist (available at <https://qims.amegroups.com/article/view/10.21037/qims-21-570/rc>).

## Methods

This prospective and observational study was conducted following the Declaration of Helsinki (as revised in 2013). It was approved by the ethics committees in our hospital and in the general hospital where the MRI scans were performed. Written informed consent was obtained from all volunteers and patients.

### Patients

This research recruited 4 volunteers to optimize the MRI protocols at the beginning of the study. A total of 68 patients with facial defects were registered to participate in the study between August 2019 and October 2020. All patients were randomly selected to have 1 MRI scan on either 7 days, 3 months, or 1 year after they underwent autologous fat graft surgery.

Of these, 21 patients canceled the surgery due to COVID-19 quarantine, 13 were excluded from the MRI examination due to geographical requirements and COVID-19 travel restrictions, and 11 patients who underwent hyaluronic acid or autologous fat injections before the study were excluded. Eventually, 23 patients were prospectively enrolled in this study.

### Surgery

The surgery included liposuction, fat preparation, and lipofilling procedures, as demonstrated in *Figure 1*. The autologous fat graft was harvested from the abdomen or thighs according to the patients' preference. Tumescence fluid containing 400 mg of lidocaine and 1 mg of

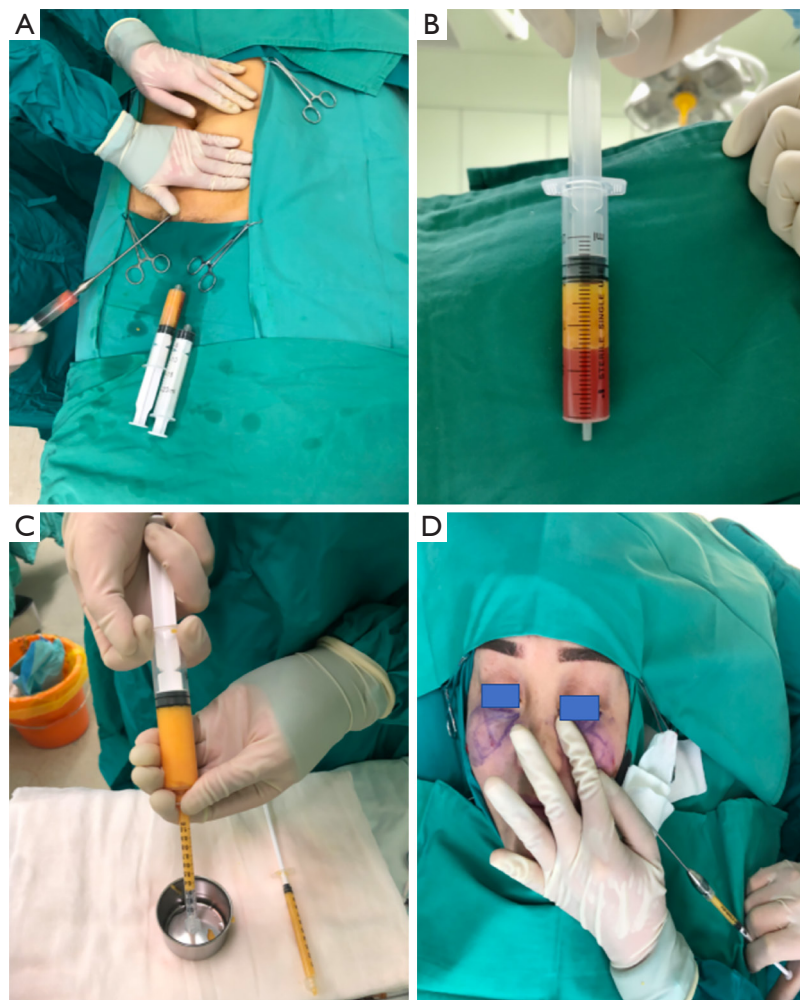


**Figure 1** Surgical procedures in a 44-year-old woman presenting for autologous fat graft injection of the face. (A) The autologous fat graft was harvested from the abdomen with a 3.0-mm sharp cannula connected to a low-pressure 20-cc syringe liposuction. (B) During fat sedimentation, the adipose cells were easily separated from the serosanguineous component. (C) Fat was then transferred into 1-mL syringes for injection. (D) Fat was injected into the deep fat layer when the syringe gradually retracted. This image is published with the patient's consent.

adrenaline per 1,000 mL of saline was infiltrated into the subcutaneous layer. Liposuction was conducted with a 3.0-mm sharp cannula connected to a low-pressure 20-cc syringe liposuction under local anesthesia. The cannula was moved back and forth to collect the autologous fat. Collected fat sedimented for about 15 minutes after rinsing. During sedimentation, the adipose cells were separated from the serosanguineous component and oils. Fat was then transferred into 1-mL syringes for injection.

Two 0.5-mm stab incisions were made on the bilateral malar or nasal sides of each patient with an 18-gauge sharp needle. The plastic surgeon injected fat into the layer of the

deep fat using an injecting cannula attached to the 1-mL syringe containing fat. For each case, the volume injected into each site was documented in the medical record.

Postoperative evaluation was performed by both the patients and the doctors and was graded as excellent, good, fair, or poor.

#### *MRI scan protocols*

A facial MRI was performed using a 3.0T unit with a 32-channel head coil (Ingenua Elition X, Philips HealthTech) to assess the facial fat signal, morphology, and

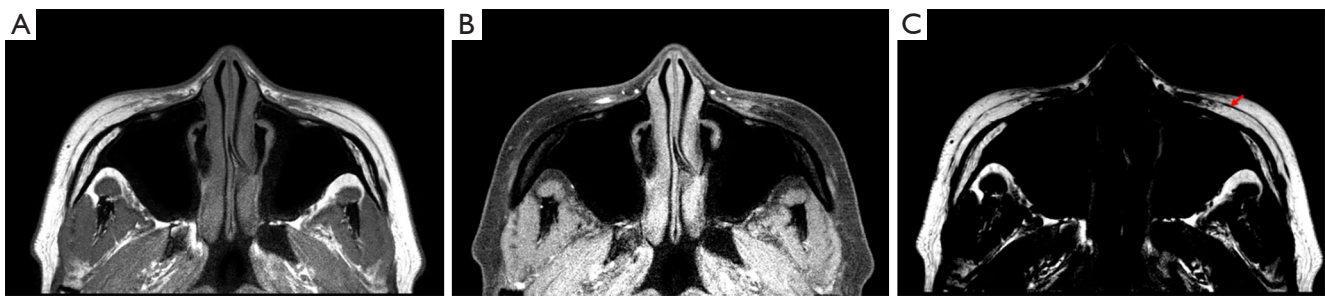


**Figure 2** Transverse noncontrast-enhanced in-phase (A), water-only (B), and fat-only (C) images of a healthy volunteer (aged 23 years, female) on bilateral malar sites. These images were acquired by a T1W 2D mDixon TSE sequence. (A) The in-phase image appears similar to a conventional TSE image. (B) The water-only image is similar to the fat-saturated image. (C) The fat-only image was generated by the mDixon imaging algorithm. Three layers are clearly displayed in the fat-only image: the first is the superficial fat layer with high signal intensity, the second is SMAS (low signal intensity, indicated by the red arrow), and the third is the deep fat layer. T1W, T1-weighted; TSE, turbo spin echo; SMAS, superficial musculo-aponeurotic system.

volume in patients. MRI was performed with submillimeter resolution to reduce the partial volume effect. These examinations were conducted 7 days, 3 months, or 1 year after surgery, and 3 sequences were applied:

A high-resolution 3D T1W Dixon with intrinsic transverse orientation was first applied; then, sagittal and coronal images were reconstructed from this 3D T1W image. These images in 3 orientations served as the fat localizer to identify the grafted fat and plan further scanning. The 3D T1W imaging was obtained with a gradient echo sequence (GRE) to achieve an acceptable signal-to-noise ratio (SNR) and scan time. Images acquired at dual echo times by a bipolar gradient readout were used for calculation of the water and fat image via the 2-point modified Dixon method (23,24).

High-resolution transverse 2D T1W and T2W Dixon TSE sequences were applied after the radiologist and surgeon identified and localized the grafted fat based on the preceding 3D sagittal and coronal images. This Dixon sequence used a dual-acquisition scheme, with an echo shift of 1 ms, to generate water-only, fat-only, and in-phase images (20) (Figure 2). Minimum bandwidth was used in the 2D DXION TSE sequences to enrich SNR. A 7-peak fat spectral model was incorporated in the Dixon imaging algorithm to improve the performance of water-fat separation (20,25-27). The detailed protocol parameters are summarized in Table 1.

### Image analysis

A radiologist with 10 years of head and neck image

reading experience and a plastic surgeon with 5 years of plastic surgery experience reviewed and analyzed all the MRI images together. They were blinded to the image sequence and time point. A 5-point Likert-type scale based on previous studies was used to qualitatively evaluate the image quality of the 2D T1W and T2W fat-only images. The image quality analysis was based on artifacts and background suppression. Another 5-point Likert-type scale was used to qualitatively assess the image differentiation between grafted fat and the surrounding native fat tissue. The 2 Likert-type scales are illustrated in Table 2. All the gradings were completed via the consensus of 2 doctors.

The contour of the grafted fat was delineated by the radiologist and confirmed by the surgeon based on the 2D T1W images, which were sharper than those of the 3D T1W. Each patient had 2 sides (left and right sides) that underwent surgeries, and information for both sides was recorded.

MR T1W and T2W images were scaled by signal receivers, amplifiers, and image reconstruction weighting factors; hence, the signal did not represent the absolute value of tissues. To address this issue, we recorded every signal in the grafted fat ( $S_i$ ) and native fat ( $S_n$ ) and calculated the relative signal contrast using Eq. [1].  $S_i$  was measured in the region-of-interest (ROI) within the grafted fat contour, while  $S_n$  was measured within an ellipse ROI larger than  $20 \text{ mm}^2$  near the grafted fat. The ROIs were chosen to avoid the edge of the patients' native fat and muscles. The grafted fat signal contrast, which is the relative difference between  $S_i$  and  $S_n$ , was calculated to quantify the difference between the signals of grafted

**Table 1** The scan parameters of the facial fat-only imaging protocols

|                                 | 3D T1W Dixon   | 2D T1W Dixon        | 2D T2W Dixon |
|---------------------------------|----------------|---------------------|--------------|
| TR (ms)                         | 12             | 606                 | 3347         |
| TE1/TE2 (ms)                    | 3.0/4.6        | 9.4 (shortest)/10.4 | 111/112      |
| Acquisition method              | GRE            | TSE                 | TSE          |
| FOV (AP/RL, mm)                 | 120/169        | 136/197             | 136/196      |
| Acquisition matrix              | 152/199        | 488/541             | 488/525      |
| Number of slices                | 250            | 30                  | 30           |
| Acquisition voxel (mm/mm/mm)    | 0.79/0.85/1.00 | 0.28/0.35/3         | 0.28/0.37/3  |
| Reconstruction voxel (mm/mm/mm) | 0.29/0.29/0.5  | 0.117/0.117/3       | 0.17/0.17/3  |
| SENSE factor                    | 1.6            | 3                   | 3            |
| Oversampling (mm)               | 8              | 10                  | 19           |
| Flip angle (°)                  | 80             | 90                  | 90           |
| Bandwidth (Hz)                  | 754.4          | 365.9               | 254.9        |
| TSE factor                      |                | 10                  | 19           |
| TSE profile order               |                | Asymmetric          | Linear       |
| Refocusing control (°)          |                | 120                 | 100          |
| NSA                             | 2              | 2                   | 2            |
| Scan duration (min:sec)         | 5:17           | 5:02                | 5:01         |

GRE, gradient echo sequence; TSE, turbo spin echo sequence; SENSE, SENSitivity Encoding; TR, time of repetition; TE, time of echo; FOV, field of view; RL, right left; AP, anterior posterior; NSA, number of signal averages.

**Table 2** The 5-point Likert-type scale in the assessment of image quality and image differentiation

| Scores   | 1 (not adequate)                         | 2 (poor)  | 3 (sufficient)   | 4 (good)   | 5 (perfect)  |
|--|--|---|--|--|--|
| Image quality  | Severe artifacts, with background signal | Major artifacts causing notable problems for image interpretation | Moderate artifacts; fat tissues are almost entirely visible  | Minor artifacts; there is some blurring of the boundary in fat tissues | No detectable artifact, excellent images; entire fat tissue visible with excellent details |
| Image differentiation between grafted fat and other fat tissue | Grafted fat could not be identified      | Poor visualization of grafted fat signal                          | Moderate visualization of grafted fat, surgical procedure information is needed for interpretation | Good visualization of grafted fat, with blurred boundary               | Clear edge between grafted fat and other tissue  |

fat and native fat.

$$\text{Signal contrast} = \frac{S_n - S_i}{S_n} \times 100\% \quad [1]$$

The contours were then copied from 2D to 3D images, interpolated into continuous contours to make more slices in the 3D T1W images, and modified if movements were observed. Following this, 3D T1W images were used to

measure the volume of grafted fat, which was measured in voxels. The measured volumes of grafted fat were then compared with the volume of injected fat, and the retention rate was calculated for each volume according to Eq. [2].

$$\text{Retention Rate} = \frac{\text{detected fat volume}}{\text{injected fat volume}} \times 100\% \quad [2]$$

**Table 3** Demographic, imaging time, and procedures of the patients

| Parameter                               | Female (n=23)   |
|---|-----------------|
| Age (years), mean $\pm$ SD              | 35 $\pm$ 7.8    |
| Ethnicity                               | Asian           |
| Time of scan after surgery              |                 |
| 7 days                                  | n=8             |
| 3 months                                | n=9             |
| 1 year                                  | n=6             |
| Donor sides                             |                 |
| Thigh                                   | n=20            |
| Abdomen                                 | n=3             |
| Bilateral recipient sides               |                 |
| Malar                                   | n=26            |
| Nasolabial                              | n=20            |
| Injected fat volume (mL, mean $\pm$ SD) | 2.60 $\pm$ 0.53 |

SD, standard deviation.

### Statistical analysis

Statistical analysis was performed with SPSS 22.0 (IBM Corp., Armonk, NY, USA). The Kruskal-Wallis test was used to compare the age of the 3 groups. The Wilcoxon signed-rank test was applied to compare image quality and image differentiation scores of 2D T1W and T2W fat-only images. An unpaired t test with Welch's correction was applied to analyze the signal contrast and volume retention rate. The Pearson correlation method was used to obtain a linear regression of the relationships between the volume of the injected fat and the measured volume of fat on postoperative day 7. The Shapiro-Wilk test was performed to test if the variables match the normal distribution. All statistical tests were 2-sided, and a P value less than 0.05 was considered statistically significant.

## Results

### Patient characteristics

With 23 female patients (age 35 $\pm$ 7.8 years) participating in the image evaluation, 46 injected sides of the face were acquired. The recipient sides of the patients were 26 at malar and 20 at the nasolabial fold. Eight patients underwent a follow-up MRI scan on postoperative day 7, 9 patients were scanned 3 months postoperatively, and 6

patients were scanned 1 year after surgery. There was no statistical difference in the age of the 3 groups ( $P=0.2$ ). The mean volume of fat grafted into each side of the face was 2.60 $\pm$ 0.53 mL. Patient satisfaction was assessed using questionnaires. Of the 23 patients, 19 (64.5%) had excellent results, 2 (22.1%) had good results, 1 (5.9%) had fair results, and 1 (7.4%) had poor results. Excellent and good results were considered to be satisfactory. In all, 21 (91.3%) patients were satisfied with the results. The postoperative clinical effect was evaluated by the doctors, yielding the following results: excellent (n=18, 78.2%), good (n=4, 17.3%), and fair (n=1, 4.3%).

To date, there have been no complications in patients. No surgical-site infections have been recorded. Three patients underwent a second injection procedure. *Table 3* shows the demographic details of patients.

### MRI and signal evaluation

The median scores of the T1W image quality and image differentiation were 5 (ranging from 4 to 5) and 5 (ranging from 4 to 5), respectively. The median scores for the T2W image quality and image differentiation were 4 (ranging from 2 to 5) and 3 (ranging from 2 to 5), respectively. There was a statistical difference between T1W and T2W for image quality ( $P<0.01$ ) and for image differentiation ( $P<0.0001$ ; *Figure 3*). *Figure 4* shows a representative case to illustrate this finding.

The mean and standard deviation of the signal contrast was 28.8% $\pm$ 4.7%, 16.33% $\pm$ 2.1%, 3.3% $\pm$ 1.3%, at 7 days, 3 months, and 1 year after the operation, respectively. There was a statistically significant difference between the postoperative follow-up after 7 days and 3 months ( $P<0.0001$ ), and between 3 months and 1 year ( $P<0.0001$ ; *Figure 5*). The MRI images showed that the injected fat of 1 patient's left side was completely absorbed 1 year after surgery; therefore, we only recorded the signal contrast of 45 sides.

### Volume measurement

In this study, Pearson correlation analysis was used to evaluate the relationship between the injected fat volume and the detected fat on day 7. There was a positive correlation between the 2 variables ( $r=0.9556$ ;  $P<0.0001$ ; *Figure 6A*), with a mean measured volume of 2.6 $\pm$ 0.47 mL and a mean retention rate of 94.1% $\pm$ 5.75% (*Figure 6B*). This indicates that the volume of the detected fat on day

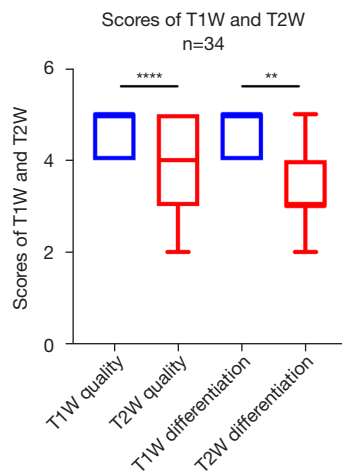


**Figure 3** Boxplots show the image quality and image differentiation scores of T1W and T2W fat-only images evaluated by the 5-point Likert-type scale. T1W scores are significantly higher than those of T2W on both variables. \*\*\*\*,  $P < 0.0001$ ; \*\*,  $P < 0.01$ ; Wilcoxon signed-rank test. T1W, T1-weighted; T2W, T2-weighted.

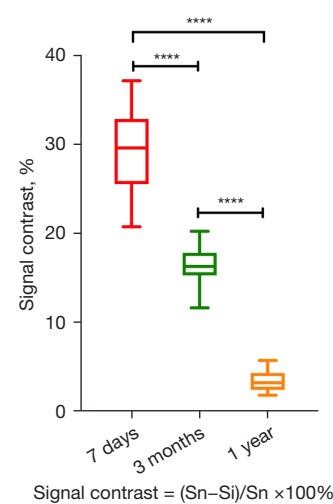


**Figure 5** Signal contrast of grafted fat on day 7, 3 months, and 1 year after surgery. Sn: signal of native fat; Si: signal of grafted fat. \*\*\*\*,  $P < 0.0001$ ; Paired  $t$  test.

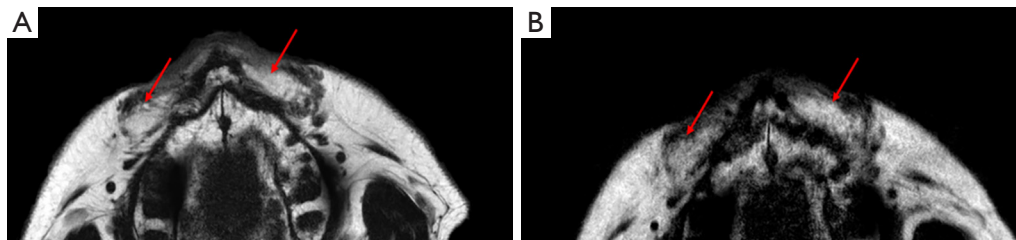


**Figure 4** Transverse noncontrast-enhanced fat-only T1W (A) and T2W (B) images of a patient (age 33 years, female) scanned 3 months after autologous fat surgery performed in bilateral nasolabial groove (red arrows). The T1W image (A) is sharper and has more contrast than the T2W image (B). T1W, T1-weighted; T2W, T2-weighted.

7 was almost equal to the volume of the injected fat that was recorded during surgery. The mean volume retention rates of the grafted fat 3 months and 1-year postoperatively were  $48.7\% \pm 17.34\%$  and  $33.1\% \pm 12.94\%$ , respectively. The volume retention rates were statistically different between 7 day and 3 months ( $P < 0.0001$ ) and between 3 months and 1 year ( $P < 0.05$ ).

## Discussion

Our study was the first of its kind to discover a significant decrease in the MRI signal contrast of grafted fat during the 1-year recovery time after a fat transfer procedure. Our

findings suggest that the content or density of injected fat was different from the native fat during this recovery time. The autologous fat signal contrast was the most obvious on day 7, and it became close to the signal of native fat tissue 1 year after surgery (Figures 5, 7).

We identified a signal intensity difference between autologous fat and native facial adipose tissue (Figure 8). As shown in Figure 8B, the autologous fat had a clumped and diffusive appearance compared to the typical lobule-like structure of native fat, and autologous fat had a lower signal intensity than did the native facial fat in the images. Therefore, this difference can be used to distinguish the grafted fat from native fat. We hypothesized that the

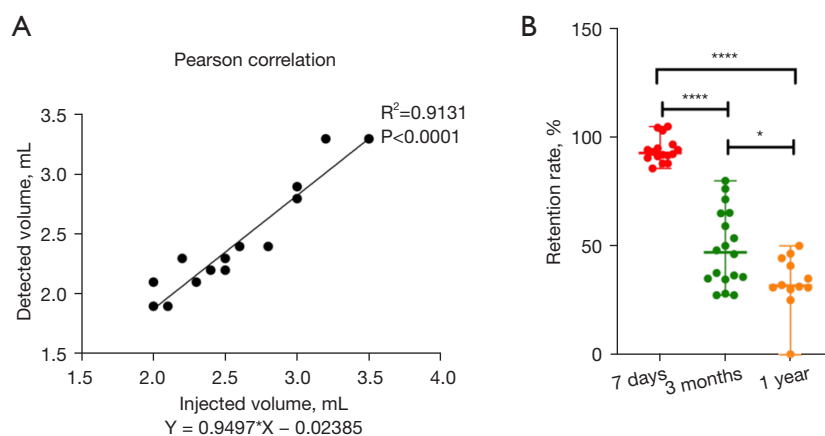


**Figure 6** Relationship between the detected and injected volume, and the volume retention rate on day 7, 3 months, and 1 year after the operation. (A) Pearson correlation analysis indicated a positive correlation between the volume of injected fat and detected fat on day 7 ( $r=0.96$ ;  $P<.0001$ ). Formula: Detected Volume =  $0.95 * \text{Injected Volume} - 0.024$  (mL). (B) Mean retention rate of injected fat on day 7 ( $94.1\% \pm 5.75\%$ ), 3 months ( $48.7\% \pm 17.34\%$ ), and 1 year ( $33.1\% \pm 12.94\%$ ) after surgery.

intracellular space of grafted fat tissue was enlarged due to inflammation and edema, which reduced fat density. Other studies have shown that the existence of collagen, which develops during the recovery process, may impact the longitudinal recovery rate of tissue and result in signal change of the autologous fat (28,29). However, these assumptions regarding chemical and biological changes have not yet been confirmed with advanced MRI methods by quantifying T1 and T2 relaxation rates or via a histologic study. Further animal studies need to be performed to make a histologic comparison of T1 and T2 changes and find the cause of grafted fat signal change in T1W and T2W images.

Normal human adipose tissue is composed of fat lobules units, which are essential for adipocyte survival. The fibrous septa anatomically separate the fat lobules, provide resistance against lobule enlargement, and offer a scaffold to which blood vessels, nerves, and lymphatics attach (30). Hence, without sufficient circulation for nutrition supply and spatial support, adipocytes in grafted fat shrink and even collapse, and are then absorbed by body (31). The septa or blood vessels are regenerated inside the grafted fat during recovery and provide support for long-term retention, and they appear to be dark lines and spots in fat-only images (30) (Figure 8). We delineated the grafted fat based on both the signal reduction and the diffuse texture, because the correct delineation could not be performed based only on the reduced signal without recognizing the texture. The grafted fat's appearance in signal and texture was close to that of

the native fat 1-year postoperation. However, we could still identify the grafted fat compared to native fat in the MRI images because of the different anatomical structures between native and grafted fat (Figure 7).

We noticed that the retention rate decreased from 3 months to 1 year after surgery, and the autologous fat signal contrast also decreased during this period. These findings showed that grafted fat volume continued to decrease from 3 months to 1 year. This is in contrast to a previous study which applied an ultrasound to calculate the retention rate after fat transfer and suggested that the volume of grafted fat would be stable 3 months after surgery (3,12). However, ultrasound imaging is limited in this application in cosmetic surgery, as the pressure applied on soft tissue changes the tissue's shape (8). Furthermore, Xie (3) arrived at a similar conclusion using patients' satisfactory questionnaires and by comparing postoperative photos with preoperative photos, but lacked an objective standard to compare patient results. In the past, MRI was only used to measure the volume of fat during fat transplantation in breasts (7). In our study, the Dixon sequence fat images were found to be sensitive to fat tissue and could distinguish grafted fat from native fat. The volume measured 7 days after surgery almost equaled the injected fat volume in all cases, which validated the accuracy of the fat-only image. Our measurements of MRI signal and volume were more quantitative and objective in characterizing the subtle change during the recovery after surgery.

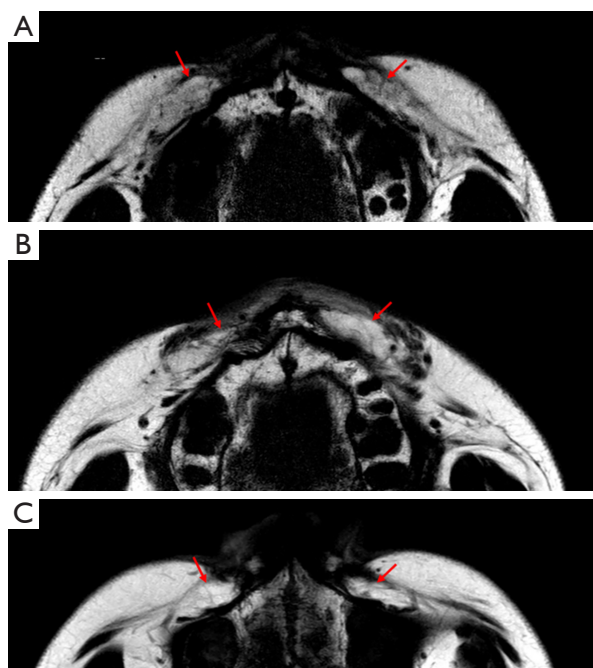


**Figure 7** Transverse noncontrast-enhanced 2D Dixon T1W fat-only images of 3 patients, each scanned at 7 days (A, aged 44, female), 3 months (B, aged 33, female), and 1 year (C, aged 40, female) after autologous fat transplantation. They all underwent the fat grafting procedure on the bilateral nasolabial grooves by the same plastic surgeon. (A) The grafted fat (red arrows) signal intensity was very low on day 7, and signal contrast between grafted fat and native facial fat was the greatest. (B) The grafted fat (red arrows) signal was stronger at 3 months, with signal contrast lower than A. (C) The relative signal of grafted fat (red arrows) compared to native adipose tissue was the strongest at 1-year postoperation, and signal contrast was the smallest. The left and right sides grafted fat retention rates were different in patients scanned at 3 months (B) and 1 year (C) after surgery. T1W, T1-weighted.

We can conclude that T1W fat-only images may be more suitable for characterizing autologous fat graft, with fewer image artifacts and better image differentiation than offered by T2W fat-only images (Figure 3). The fat-only T2W TSE sequence was more prone to motion artifacts, like other applications of T2W TSE. Also, regarding lower image differentiation in T2W images, the T2W Dixon imaging sequence was not optimized for fat-only images with the currently implemented TE (time of echo) because the fat transverse relaxation rate T2 is much longer than the T2 of water.

Various techniques have been developed to assess fat

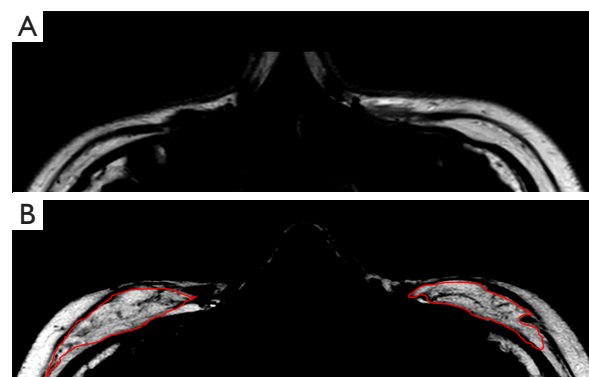


**Figure 8** Transverse fat-only images after autologous fat grafting performed in bilateral malar sites. (A) A transverse view of fat-only image of a normal volunteer. Three layers are clearly displayed in the fat-only image. (B) The transferred autologous fat (red lines) signal intensity is lower than the native adipose tissue, and its texture is diffuse, based on which the transferred autologous fat can be identified.

graft retention during postoperative management and to identify possible predictive factors of this retention. However, previous studies based on CT (13), conventional MRI (1,4,7,32), 3D volumetric surface imaging (33), and ultrasound imaging (1,12) found it challenging to characterize the small amount of facial grafted fat (8,11,12). The fat-only images generated by Dixon imaging have excellent image quality, which can directly measure the amount of grafted fat in patients and provide a full anatomical structure of adipose tissue. The fat-only images were also used to guide the second injection procedures for the 3 patients who underwent second autologous fat transfer.

In the past, patients needed to have comparative scans before and after operations to measure the augmented fat volume (12). Our study found that the fat-only images could clearly delineate grafted fat from native fat on day 7, so a preoperational scan could be unnecessary. Scans of the patients 1 year postoperatively also found there to be no difference between the grafted fat signal and the native fat signal ( $P=0.43$ ). Further observational experiments need to be conducted to investigate if the volume of grafted fat continues to shrink after 1 year.

Our study had several limitations. The number of participants was low, and not all of the same participants were scanned at all 3 follow-up times. No evaluations were performed to see if any changes of the grafted fat occurred after 1 year. Furthermore, the size of the anatomy under investigation was small; therefore, the partial volume effect

could cause flaws in measuring the grafted fat signal and reference signal, so sampling ROIs need to avoid the edges of fat tissue to reduce potential bias.

## Conclusions

Based on the fat-only images, we confirmed that the grafted fat signal significantly differed from the native facial fat signal, and the signal contrast and volume gradually decreased during the 1-year recovery time after the fat transfer procedure. T1W fat-only images obtained by Dixon imaging displayed grafted fat more effectively than T2W, with sufficient image quality and image differentiation for grafted fat delineation and volume measurements.

## Acknowledgments

The authors would like to thank Xiaofang Xu, the RT for MRI protocol adjustment. His consent was obtained to be cited, and he agreed with the data and conclusions of the study.

*Funding:* None.

## Footnote

*Reporting Checklist:* The authors have completed the MDAR checklist. Available at <https://qims.amegroups.com/article/view/10.21037/qims-21-570/rc>

*Conflicts of Interest:* All authors have completed the ICMJE uniform disclosure form (available at <https://qims.amegroups.com/article/view/10.21037/qims-21-570/coif>). XW is employed by Philips, China. The other authors have no conflicts of interest to declare.

*Ethical Statement:* The authors are accountable for all aspects of the work in ensuring that questions related to the accuracy or integrity of any part of the work are appropriately investigated and resolved. The study was conducted in accordance with the Declaration of Helsinki (as revised in 2013), and informed consent was obtained from all individual participants. This study was approved by the ethics committees in our hospital and in the general hospital where MRI scans were performed.

*Open Access Statement:* This is an Open Access article distributed in accordance with the Creative Commons Attribution-NonCommercial-NoDerivs 4.0 International

License (CC BY-NC-ND 4.0), which permits the non-commercial replication and distribution of the article with the strict proviso that no changes or edits are made and the original work is properly cited (including links to both the formal publication through the relevant DOI and the license). See: <https://creativecommons.org/licenses/by-nc-nd/4.0/>.

## References

1. Shim YH, Zhang RH. Literature Review to Optimize the Autologous Fat Transplantation Procedure and Recent Technologies to Improve Graft Viability and Overall Outcome: A Systematic and Retrospective Analytic Approach. *Aesthetic Plast Surg* 2017;41:815-31.
2. Ma X, Wu L, Ouyang T, Ge W, Ke J. Safety and Efficacy of Facial Fat Grafting Under Local Anesthesia. *Aesthetic Plast Surg* 2018;42:151-8.
3. Xie Y, Li Q, Zheng D, Lei H, Pu LL. Correction of hemifacial atrophy with autologous fat transplantation. *Ann Plast Surg* 2007;59:645-53.
4. Lin DJ, Wong TT, Ciavarra GA, Kazam JK. Adventures and Misadventures in Plastic Surgery and Soft-Tissue Implants. *Radiographics* 2017;37:2145-63.
5. Denadai R, Raposo-Amaral CA, Raposo-Amaral CE. Fat Grafting in Managing Craniofacial Deformities. *Plast Reconstr Surg* 2019;143:1447-55.
6. Wolf GA, Gallego S, Patrón AS, Ramírez F, de Delgado JA, Echeverri A, García MM. Magnetic resonance imaging assessment of gluteal fat grafts. *Aesthetic Plast Surg* 2006;30:460-8.
7. Spear SL, Pittman T. A prospective study on lipoaugmentation of the breast. *Aesthet Surg J* 2014;34:400-8.
8. Cansanco AL, Condé-Green A, David JA, Vidigal RA. Subcutaneous-Only Gluteal Fat Grafting: A Prospective Study of the Long-Term Results with Ultrasound Analysis. *Plast Reconstr Surg* 2019;143:447-51.
9. Masarapu V, Wang PS, Gorbachova T. Slow-growing buttock mass after failure of incorporation of autologous fat transfer for gluteal augmentation: ultrasound and MRI features. *Skeletal Radiol* 2020;49:1669-75.
10. Osswald R, Boss A, Lindenblatt N, Vorburger D, Dedes K. Does lipofilling after oncologic breast surgery increase the amount of suspicious imaging and required biopsies?-A systematic meta-analysis. *Breast J* 2020;26:847-59.
11. Gerth DJ, King B, Rabach L, Glasgold RA, Glasgold MJ. Long-term volumetric retention of autologous fat grafting processed with closed-membrane filtration. *Aesthet Surg J*

- 2014;34:985-94.
12. Denadai R, Raposo-Amaral CA, Pinho AS, Lameiro TM, Buzzo CL, Raposo-Amaral CE. Predictors of Autologous Free Fat Graft Retention in the Management of Craniofacial Contour Deformities. *Plast Reconstr Surg* 2017;140:50e-61e.
  13. Cotofana S, Gotkin RH, Frank K, Koban KC, Targosinski S, Sykes JM, Schlager M, Schlattau A, Schenck TL. The Functional Anatomy of the Deep Facial Fat Compartments: A Detailed Imaging-Based Investigation. *Plast Reconstr Surg* 2019;143:53-63.
  14. Glover GH, Schneider E. Three-point Dixon technique for true water/fat decomposition with B0 inhomogeneity correction. *Magn Reson Med* 1991;18:371-83.
  15. Berglund J, Ahlström H, Johansson L, Kullberg J. Two-point dixon method with flexible echo times. *Magn Reson Med* 2011;65:994-1004.
  16. Eggers H, Börnert P. Chemical shift encoding-based water-fat separation methods. *J Magn Reson Imaging* 2014;40:251-68.
  17. Noble JJ, Keevil SF, Totman J, Charles-Edwards GD. In vitro and in vivo comparison of two-, three- and four-point Dixon techniques for clinical intramuscular fat quantification at 3 T. *Br J Radiol* 2014;87:20130761.
  18. Guerini H, Omoumi P, Guichoux F, Vuillemin V, Morvan G, Zins M, Thevenin F, Drape JL. Fat Suppression with Dixon Techniques in Musculoskeletal Magnetic Resonance Imaging: A Pictorial Review. *Semin Musculoskelet Radiol* 2015;19:335-47.
  19. Ji X, Huang W, Dong H, Shen Z, Zheng M, Zou D, Shen W, Xia S. Evaluation of bone marrow infiltration in multiple myeloma using whole-body diffusion-weighted imaging and T1-weighted water-fat separation Dixon. *Quant Imaging Med Surg* 2021;11:641-51.
  20. Dixon WT. Simple proton spectroscopic imaging. *Radiology* 1984;153:189-94.
  21. Kovanlikaya A, Mittelman SD, Ward A, Geffner ME, Dorey F, Gilsanz V. Obesity and fat quantification in lean tissues using three-point Dixon MR imaging. *Pediatr Radiol* 2005;35:601-7.
  22. Fischer MA, Pfirrmann CW, Espinosa N, Raptis DA, Buck FM. Dixon-based MRI for assessment of muscle-fat content in phantoms, healthy volunteers and patients with achillogdynia: comparison to visual assessment of calf muscle quality. *Eur Radiol* 2014;24:1366-75.
  23. Xiang QS. Two-point water-fat imaging with partially-opposed-phase (POP) acquisition: an asymmetric Dixon method. *Magn Reson Med* 2006;56:572-84.
  24. Eggers H, Brendel B, Duijndam A, Herigault G. Dual-echo Dixon imaging with flexible choice of echo times. *Magn Reson Med* 2011;65:96-107.
  25. Wehrli FW. Chemical shift-induced amplitude modulations in images obtained with gradient refocusing. *Magnetic Resonance Imaging* 1987;5:157-8.
  26. Ren J, Dimitrov I, Sherry AD, Malloy CR. Composition of adipose tissue and marrow fat in humans by 1H NMR at 7 Tesla. *J Lipid Res* 2008;49:2055-62.
  27. Kijowski R, Woods MA, Lee KS, Takimi K, Yu H, Shimakawa A, Brittain JH, Reeder SB. Improved fat suppression using multipeak reconstruction for IDEAL chemical shift fat-water separation: application with fast spin echo imaging. *J Magn Reson Imaging* 2009;29:436-42.
  28. Silva ABD, Haupenthal F, Morais AD, Ascenço ASK, Sebastião APM, Cavalcanti MAR, Freitas RS. Relationship between Tamoxifen and the Absorption of Subfascial Autologous Fat Grafts. *Plast Reconstr Surg* 2018;141:1408-15.
  29. Kuroiwa Y, Yamashita A, Miyati T, Furukoji E, Takahashi M, Azuma T, Sugimura H, Asanuma T, Tamura S, Kawai K, Asada Y. MR signal change in venous thrombus relates organizing process and thrombolytic response in rabbit. *Magn Reson Imaging* 2011;29:975-84.
  30. Sun W, Fang J, Yong Q, Li S, Xie Q, Yin J, Cui L. Subcutaneous Construction of Engineered Adipose Tissue with Fat Lobule-Like Structure Using Injectable Poly-Benzyl-L-Glutamate Microspheres Loaded with Adipose-Derived Stem Cells. *PLoS One* 2015;10:e0135611.
  31. Patrick CW. Breast tissue engineering. *Annu Rev Biomed Eng* 2004;6:109-30.
  32. Skorobac Asanin V, Sopta J. Lower Leg Augmentation with Fat Grafting, MRI and Histological Examination. *Aesthetic Plast Surg* 2017;41:108-16.
  33. Schreiber JE, Stern CS, Jelks EB, Jelks GW, Tepper OM. Three-Dimensional Topographic Surface Changes in Response to Volumization of the Lateral Suborbicularis Oculi Fat Compartment. *Plast Reconstr Surg* 2020;145:653-9.

**Cite this article as:** Liao X, Wang X, Xu Z, Guo S, Gu C, Jin Z, Su T, Chen Y, Xue H, Yang M. Assessment of facial autologous fat grafts using Dixon magnetic resonance imaging. *Quant Imaging Med Surg* 2022;12(5):2830-2840. doi: 10.21037/qims-21-570